

An FT-IR Study on Packing Defects in Mixed β -Aggregates of Poly(L-glutamic acid) and Poly(D-glutamic acid): A High-Pressure Rescue from a Kinetic Trap

Yudai Yamaoki,^{†,‡} Hiroshi Imamura,[‡] Aleksandra Fulara,[†] Sławomir Wójcik,[†] Łukasz Bożycki,^{§,||} Minoru Kato,[‡] Timothy A. Keiderling,[⊥] and Wojciech Dzwolak^{*,†}

[†]Department of Chemistry, University of Warsaw, Pasteura 1, 02-093 Warsaw, Poland

[‡]Department of Pharmacy, Ritsumeikan University, 1-1-1 Noji-higashi, Kusatsu, Shiga 525-8577, Japan

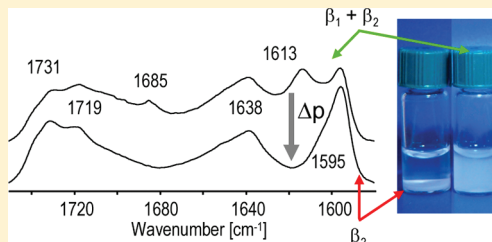
[§]Warsaw University of Life Sciences, Nowoursynowska 166, 02-787 Warsaw, Poland

^{||}Institute of High Pressure Physics, Polish Academy of Sciences, Sokolowska 29/37, 01-142 Warsaw, Poland

[⊥]Department of Chemistry, University of Illinois at Chicago, 845 West Taylor Street (m/c 111), Chicago, Illinois 60607-7061, United States

S Supporting Information

ABSTRACT: Under favorable conditions of pH and temperature, poly(L-glutamic acid) (PLGA) adopts different types of secondary and quaternary structures, which include spiral assemblies of amyloid-like fibrils. Heating of acidified solutions of PLGA (or PDGA) triggers formation of β_2 -type aggregates with morphological and tinctorial properties typical for amyloid fibrils. In contrast to regular antiparallel β -sheet (β_1), the amide I' vibrational band of β_2 -fibrils is unusually red-shifted below 1600 cm^{-1} , which has been attributed to bifurcated hydrogen bonds coupling C=O and N-D groups of the main chains to glutamic acid side chains. However, unlike for pure PLGA, the amide I' band of aggregates precipitating from racemic mixtures of PLGA and PDGA (β_1) is dominated by components at 1613 and 1685 cm^{-1} —typically associated with intermolecular antiparallel β -sheets. The coaggregation of PLGA and PDGA chains is slower and biphasic and leads to less-structured assemblies of fibrils, which is reflected in scanning electron microscopy images, sedimentation properties, and fluorescence intensity after staining with thioflavin T. The β_1 -type aggregates are metastable, and they slowly convert to fibrils with the infrared characteristics of β_2 -type fibrils. The process is dramatically accelerated under high pressure. This implies the presence of void volumes within structural defects in racemic aggregates, preventing the precise alignment of main and side chains necessary to zip up ladders of bifurcated hydrogen bonds. As thermodynamic costs associated with maintaining void volumes within the racemic aggregate increase under high pressure, a hyperbaric treatment of misaligned chains leads to rectifying the packing defects and formation of the more compact form of fibrils.



INTRODUCTION

Amyloid fibrils are linear β -sheet-rich aggregates of misfolded protein molecules. The presence of amyloid deposits in animal tissues is often associated with an onset of degenerative maladies such as Alzheimer's disease, Parkinson's disease, or diabetes mellitus type II.¹ Many proteins, which are not observed to misfold and aggregate *in vivo*, convert nevertheless to amyloid fibrils *in vitro* upon incubation under partly denaturing conditions.^{2,3} By now, dozens of clinical conditions have been linked to the formation of amyloid fibrils.⁴ On the other hand, considerable evidence suggesting that amyloid fibrils may play nonpathogenic biological functions has been gathered as well.^{5–7} Moreover, there are many examples of possible applications of “functional” amyloid fibrils in nanotechnology, plasmonics, and medicine.^{8–11} The trend to employ amyloids as building blocks for advanced functional materials and molecular devices is facilitated by the fact that

amyloid-like fibrils may be obtained not only from misfolded globular proteins but also from short synthetic peptides or sequenceless polymerized α -amino acids such as poly(L-lysine) or poly(L-glutamic acid).^{12,13} Namely, the chemical uniformity of side chains favors applications of homopolypeptides as effective and tunable scaffolds for functionalization with organic molecules and metal nanoparticles.^{14,15}

Aggregation of PLGA is particularly interesting as it may lead to two different types of β -fibrils (termed β_1 and β_2) with quite distinct spectral features in the vibrational amide I band (or “I’ band” for deuterated protein backbone). Infrared spectra of β_1 fibrils exhibit features typical for an intramolecular antiparallel β -sheet with the amide I’ band split into a pair of strong and

Received: December 29, 2011

Revised: March 18, 2012

Published: April 16, 2012

weak components at 1616 and 1683 cm^{-1} , respectively.¹² However, the amide I' band of the β_2 fibrils is dramatically downshifted below 1600 cm^{-1} , a value not observed for proteins. The two forms were first described by Itoh and colleagues in the 1970s in an elegant study employing X-ray diffraction and infrared absorption spectroscopy.¹⁶ We have recently revisited these findings in the contemporary context of amyloidogenicity of PLGA.¹⁷ Our studies suggested that an unusual pattern of three-center hydrogen bonds with bifurcated peptide bonds' carbonyl acceptors may underlie the extreme red-shift of the amide I' band. In a following study, we concluded that these spectral features correlate with the presence of superstructural arrangements of individual PLGA fibrils and strong enhancement of the amide I' vibrational circular dichroism which decreases sharply when packing defects appear in the fibrous scaffold.¹⁸ This observation has led us to realize that β -fibrils of poly(glutamic acid) may be used as a very sensitive model for investigating influence of packing defects on spectral properties and stability of amyloid superstructures. In particular, this holds true for high-pressure effects on amyloid fibrils—an important problem from the perspectives of both fundamental and applied research. Packing defects introduce void volumes into the densely compacted 3D structure of fibrils, rendering them vulnerable to high hydrostatic pressure.¹⁹ In fact, apart from pressure-sensitive hydrophobic and electrostatic interactions,²⁰ void volumes are thought to be one of the three main structural features conducive to protein denaturation under high pressure.^{21,22} Hence, on the one hand, a high-pressure treatment provides means to probe water-excluded cavities within amyloid fibrils; on the other hand, it may constitute an effective route for dissociation and denaturation of pathogenic protein aggregates,²³ as has been shown in the case of the high-pressure-induced inactivation of prion infectivity.^{24,25} In this context, the β_1 and β_2 aggregates of poly(glutamic acid) can be viewed as insightful model systems to investigate role of packing defects in pressure-induced transitions of protein aggregates and dynamics of self-assembling polypeptides. This knowledge is critical not only for development of high-pressure methods of eradication of proteinaceous pathogens but also for advancing pressure-tuned approaches to self-assembly of proteins for nanotechnology-oriented applications.^{26,27}

MATERIALS AND METHODS

Samples. PLGA (catalog number P4761, lot 096 K5103) and PDGA (catalog number P4033, lot 097HS907) as sodium salts (MW 15–50 kDa) were obtained from Sigma. We have paid special attention to homogeneity and linearity of polypeptide samples, as both broad MW distribution and branching could prevent proper folding and packing of secondary structures. SEC was used to assess quality of commercial samples (see Supporting Information).

The typical routine for preparation of PLGA/PDGA β -sheet-rich aggregates consisted of dissolving the respective sodium salts of poly(glutamic acid) in D_2O at the 1 wt % concentration and subsequent acidification with diluted DCl to $\text{pD} \sim 4.3$ (uncorrected for isotopic effects), as described earlier.^{17,18}

For preparation of mixed (PLGA and PDGA) aggregates, first poly(glutamic acid) solutions (1 wt %) were prepared separately from each enantiomer at neutral pD . Subsequently, both the solutions were mixed at the desired proportions and then vortexed for 30 min before they were pD -adjusted. Aggregates were prepared through incubation of freshly

acidified polypeptide samples for varying periods of time at 65 °C. Samples for Raman, SEM, and HP FT-IR analysis were obtained through a 24 h long incubation at 65 °C. D_2O and DCl were obtained from ARMAR Chemicals, Switzerland, while ThT was from Sigma.

FT-IR Spectroscopy. For ambient pressure FT-IR measurements, a CaF_2 transmission cell equipped with 25 μm Teflon spacers was used. Infrared spectra were collected on a Nicolet NEXUS FT-IR spectrometer equipped with a liquid nitrogen-cooled MCT detector at 2 cm^{-1} resolution. During measurements the sample chamber was continuously purged with dry CO_2 -depleted air. Typically, for a single spectrum, 256 interferograms were coadded. Each sample spectrum was corrected by subtracting the correct amount of D_2O and water vapor spectra. Spectra were baseline-corrected and then normalized by the integrated intensity of the amide I' band. Data processing was performed using GRAMS software (ThermoNicolet). All further experimental details were the same as specified earlier.^{17,28}

High-Pressure FT-IR Spectroscopy. High-pressure FT-IR spectroscopy employing diamond anvil cells is a powerful technique enabling monitoring *in situ* changes induced in protein secondary structure by high hydrostatic pressure.²⁹ We used a homemade diamond anvil cell with ZnSe condensers and BaSO_4 as a pressure calibrant. Measurements at 25 and 65 °C, as indicated in the figure captions, were carried out using a JASCO FT/IR-680 plus spectrometer. Pressure in the diamond anvil cell was increased at the average rate of $\sim 100 \text{ MPa/h}$. All other details were the same as specified in our earlier works.^{30–32}

High-Pressure Incubation of Samples. Incubation of samples of aggregates was carried out at 1 GPa pressure and at 25 °C using a high-pressure apparatus from UNIPRESS, Poland.²⁸

ThT Fluorescence Measurements. ThT fluorescence measurements were carried out under typical conditions.¹⁰ Namely, 0.3 wt % aqueous stock solution of ThT was added to a 10 times diluted stock PLGA sample ($\text{pH} \sim 4$) to the final concentration of the dye 25 μM . Fluorescence of ThT-stained aggregates was excited at 450 nm and measured on an AMINCO Bowman Series 2 luminescence spectrometer.

Scanning Electron Microscopy. For SEM imaging, droplets of aqueous suspensions of aggregates were deposited on silicon wafers and dried under vacuum ($\sim 0.05 \text{ mbar}$) at room temperature. Films of fibrils were sputtered with $\sim 40 \text{ nm}$ thick layers of Au/Pd alloy before SEM images were collected on a Zeiss Leo 1530 microscope.

RESULTS AND DISCUSSION

Influence of changing the PLGA/PDGA ratio on properties of the resulting β -pleated coaggregates of poly(glutamic acid)s as obtained after a 48 h long incubation at 65 °C is reported in Figure 1. As the infrared spectra in the top panel (Figure 1A) show, aggregated enantiomerically pure PLGA (or PDGA) gives rise to a pair of sharp and unusually red-shifted peaks in the spectral region corresponding to the amide I' vibrational band. The signals at 1731/1719 cm^{-1} are assigned to stretching vibrations of Glu –COOD groups. We have proposed earlier that the 1595 cm^{-1} peak is the lower, more intense component of a strongly exciton split β -structure amide I' band,^{17,18} whose upper component is probably at around 1650 cm^{-1} . In a typical antiparallel β -sheet, these appear at approximately 1616 and 1683 cm^{-1} , respectively.¹² Such an assignment suggests that the

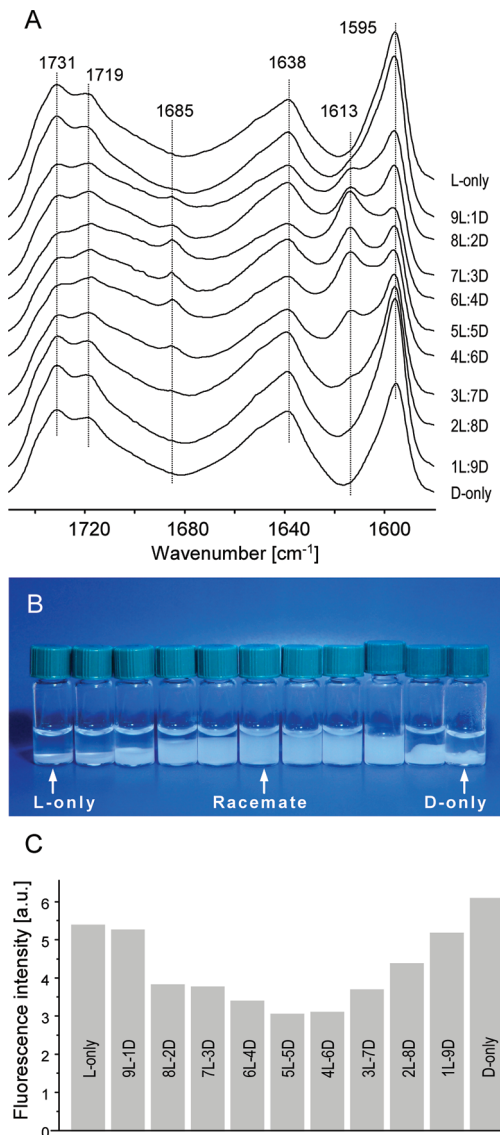


Figure 1. FT-IR spectra of samples of mixed PLGA and PDGA at varying L:D molar ratios, pD 4.3, incubated at 65 °C for 48 h. The total polypeptide concentration was 1 wt % (A). An image of the samples taken afterward reveals different sedimentation properties of aggregates depending on the L:D ratio—PDGA concentration increases gradually from the left to the right (B). Corresponding intensities of fluorescence at 480 nm of the samples stained with ThT (C).

1638 cm⁻¹ band would correspond to the Raman allowed transition, which we have verified separately (ref 18; see also Supporting Information). Therefore, the minor exciton split component of antiparallel β_2 -sheet is likely to be obscured by the strong 1638 cm⁻¹ band (although still visible at its shoulder at 1650 cm⁻¹; Figure 1A). The powerful frequency shift of the amide I' band has been attributed primarily to the formation of unusual bifurcated hydrogen bonds coupling peptide's C=O and N—D (N—H) groups of the main chain to —COOD (—COOH) groups of Glu side chains.^{17,18} Direct proximity of glutamic acid side chains to the neighboring main chains is required to form such three-center hydrogen bonds, and this seems to be fulfilled in light of the packing model of β_2 aggregates of PLGA based on X-ray diffraction data.¹⁶ Formation of this bonding pattern would lead to a net gain

in hydrogen bonds strength and a consequent net reduction of the force constant of C=O stretch. The ensuing infrared spectra of aggregates precipitating from mixed solutions of PLGA and PDGA (Figure 1A) indicate that with the [PLGA]:[PDGA] ratio approaching 1, a pair of new peaks at 1685 and 1613 cm⁻¹ gradually emerges, while intensities of the 1638 and 1595 cm⁻¹ bands become somewhat attenuated. These 1685/1613 cm⁻¹ peaks are the usual hallmark of intermolecular antiparallel β -sheet involving typical cross-strand hydrogen bonds (β_1 -aggregate). A likely explanation for the fact that the most pronounced spectral changes do not coincide exactly with the racemic composition of the aggregate, but rather with a tiny excess of PLGA is that the commercially accessible samples of PLGA and PDGA used in this study are not entirely equivalent (in terms of MW, possibly also in terms of branching of main chains and covalent modifications of side chains; see Supporting Information). We have made similar observations in our previous work.¹⁸ Interestingly, the tiniest concentrations of chiral “impurities” (PLGA/PDGA ratios 1:9 and 9:1; Figure 1A) appear to be accommodated within the β_2 structure without any detectable evidence of β_1 .

The photographic image taken with liquid samples of mixed aggregates obtained after 48 h of quiescent incubation at 65 °C (Figure 1B) reveals an unequivocal correlation between the formation of β_2 -type aggregates and a higher sedimentation rate. Furthermore, fluorescence emission of these samples after staining with thioflavin T—an amyloid-specific fluorophore probe—increases with the relative proportion of the β_2 form (Figure 1C).

Upon incubation at 65 °C, α -helical conformation of poly(glutamic acid) transforms into aggregated β -sheets involving either three-center (β_2) or two-center (β_1) hydrogen bonds. In a generalized case, the varying sedimentation properties could originate from a number of physicochemical factors, e.g., uncompensated surface charges or varying hydrophobicity of polypeptide's chemical groups. However, given the chemical composition of this particular system, the most likely reason is that pure PLGA (or PDGA) forms tightly packed particles, which are depleted of void volumes or internal water-filled cavities, which would reduce average density of aggregates while increasing their buoyancy, as is the case of β_1 -precipitates formed in solutions of mixed PLGA and PDGA. The decrease of ThT fluorescence emission shown in Figure 1C could indicate that the β_1 form is less structured on the superconformational level. This would be expected for an amorphous aggregate lacking ordered stacks of β -strands which have the capacity to tightly bind ThT molecules, restrict freedom of their intramolecular rotation, and consequently increase the ThT quantum yield of fluorescence by orders of magnitude.³³

SEM images of aggregates precipitating from acidified solutions of PLGA, PDGA, and their racemic mixtures shown in Figure 2 clearly support the hypothesis that the coassembly of PLGA and PDGA yields less ordered structures. While the enantiomerically pure polypeptide aggregates form spiral-like superstructures with a handedness reflecting the chirality of monomer amino acids (i.e., left-handed spirals for PLGA and right-handed for PDGA),¹⁸ on this level of structural assembly, the racemate is amorphous. However, linking the lower ThT emission from the mixed PLGA + PDGA aggregates to their structural disorder (Figure 1C) is not straightforward given the fact that poly(glutamic acid) does form amyloid-like fibrils with the infrared characteristics very similar to the racemic aggregate.

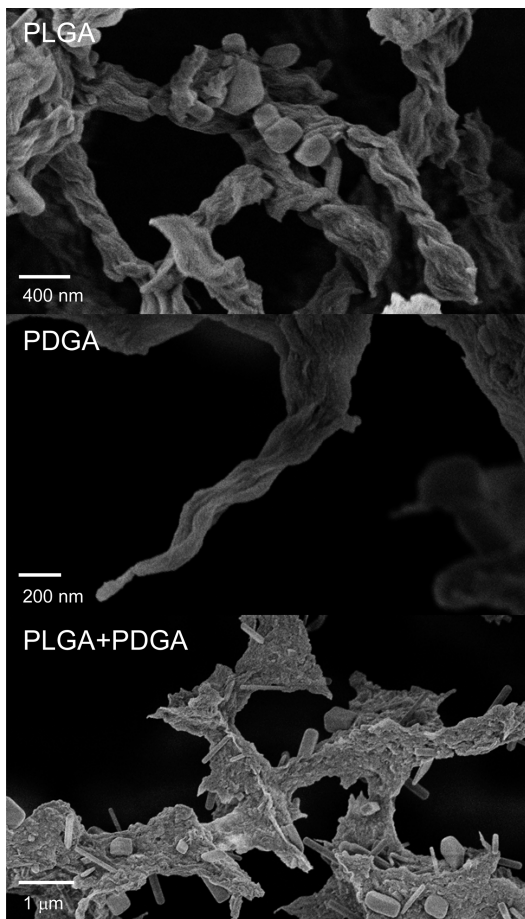


Figure 2. SEM images of mature aggregates of PLGA, PDGA, and a racemic mixture of both polypeptides. The tiny regular forms correspond to crystalline inclusions of salts.

Fändrich and Dobson observed highly regular amyloid fibrils (and no evidence of amorphous aggregates) in PLGA samples with the corresponding two main components of the amide I' band at 1616 and 1683 cm^{-1} .¹² In our recent study, we showed TEM evidence of dispersed fibrils in racemic aggregates of PLGA and PDGA.¹⁸ Such individual fibrils are still amyloid-like, although they are apparently unable to merge into ordered spiral superstructures visible in SEM. In other words, the observed structural disorder in the PLGA + PDGA aggregates does not occur on the level of polypeptide's conformation or morphology of protofilaments, but rather on the higher "superfibrillar" level. Therefore, it seems plausible that more subtle effects may underlie the negative correlation between intensity of ThT fluorescence and the β_1/β_2 ratio. The quantum yield of ThT fluorescence strongly depends on the intramolecular twist of the dye or, more precisely, on the dihedral angle around the single bond linking ThT molecule's benzothiazole and benzaminic rings.^{34,35} Upon docking of ThT onto an amyloid surface, the twist of the local fluorophore-binding moiety will constrain the ThT conformation.^{36,37} Hence, a varying degree of the surface twisting of amyloid fibrils in β_1 and β_2 samples may underlie the trend observed in Figure 1C.

Time-lapse FT-IR spectra of poly(glutamic acid) undergoing the α -helix-to- β -sheet conformational transition at 65 °C provide a direct insight into mechanisms of formation of β_1 - and β_2 -type aggregates. Upon prolonged heating of racemic mixtures of PLGA and PDGA at pH 4.1, pair of peaks at 1613

and 1685 cm^{-1} corresponding to β_1 -sheets gradually emerge at the expense of the 1640 cm^{-1} component that can be assigned to solvated α -helices which dominate at low temperature (Figure 3A).³⁸ Interestingly, even before the α -to- β_1 transition

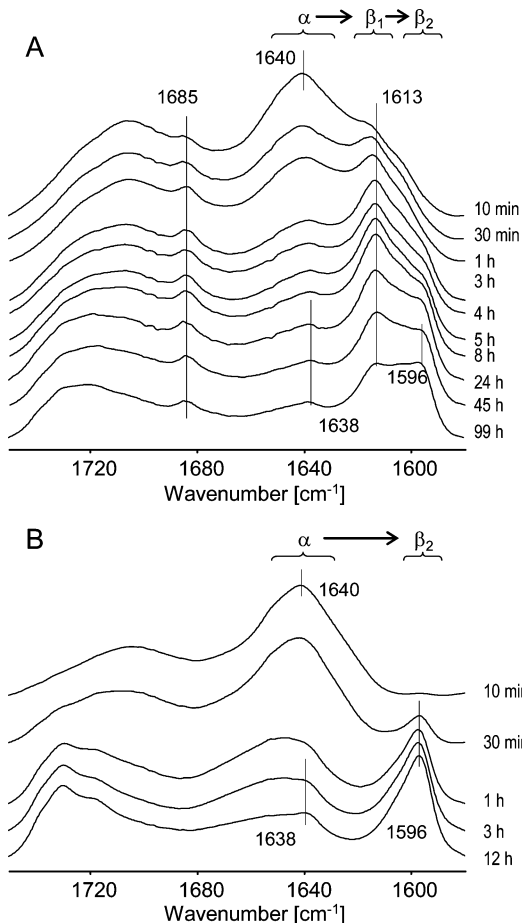


Figure 3. Time-dependent changes in FT-IR spectra of racemic mixture of α -helical PLGA and PDGA (A) and of pure PLGA (B). The samples were prepared in D_2O , acidified, and then incubated at 65 °C for the periods indicated in the figure.

is completed, within the first 4 h of high-temperature incubation of the racemate, the 1596/1638 cm^{-1} components associated with the β_2 -type aggregate are becoming visible. The continuing β_1 -to- β_2 transition is very slow and is not complete even after 99 h of incubation. This is in stark contrast to kinetics of aggregation of PLGA reported in Figure 3B. For the pure enantiomer, the transition does not proceed through any distinct intermediate states and is complete within 12 h of incubation at 65 °C. This observation contradicts earlier studies suggesting that aggregation of pure PLGA (taking place under similar conditions) would produce aggregates with the β_1 -like infrared characteristics.^{12,16} Our interpretation of this puzzle is that as long as PLGA chains are linear and free from covalent defects, the unperturbed temperature-induced transition will lead straight to β_2 aggregate. We have carried out a thorough characterization of PLGA and PDGA (Supporting Information) which proved that the lots of PLGA and PDGA used in this study are, within the accuracy of these methods, linear. At this point, we may only speculate that sporadic branching, covalent modifications of side chains, or even a higher degree of heterogeneity of some commercially accessible PLGA samples

could evoke packing defects resulting in aggregates with the infrared traits resembling those of β_1 -fibrils.

The different scenarios of aggregation of single and mixed enantiomers of poly(glutamic acid) apparent in Figure 3 strongly suggest that β_2 aggregate is thermodynamically stable, while β_1 -type is a kinetically trapped state. Importantly, the polypeptide is soluble only in the initial α -helical form, while either α/β_2 or $\alpha/\beta_1/\beta_2$ conformational transitions are coupled to the phase transition (precipitation). Obviously, subsequent conformational changes in a once-formed insoluble phase are significantly decelerated, as is the case of the ultimate conversion of β_1 to β_2 . The fact that strong bifurcated HBs maintain the thermodynamically favorable form implies that the relative stability of β_2 is, at least in part, enthalpic in origin. Certainly, the tight packing of glutamic acid side chains within the bulk β_2 precipitate reduces total surface accessible area of charge-depleted (at low pD) polypeptide chains, and this could prove to be an additional stabilizing factor. During the aggregation in racemic samples, spontaneous formation of the first interchain hydrogen bonds (following thermal destabilization of α -helices) is likely to be a random event that takes place between chains of opposite as well as identical chiral types. Hypothetically, a dense network of such heterogeneous local contacts could act as a kinetic trap preventing the polypeptide's main and side chains from establishing bifurcated hydrogen bonds that could be accommodated within a higher-order structure. This is, however, entirely at odds with the behavior of another amyloidogenic homopolymer—polylysine—for which formation of racemic aggregates of mixed poly(L-lysine) and poly(D-lysine) is not only faster but also thermodynamically preferred.¹³ At this stage, it is unclear why the two poly(α -amino acid)s behave so differently.

The physicochemical properties of β_1 and β_2 aggregates of poly(glutamic acid) and the distinct chronology of conformational events accompanying their formation have led us to conclude that the β_2 aggregate is the thermodynamically stable, tightly packed and defect-free structure, while β_1 is metastable and partly disordered, at least on the mesoscopic scale. Structural packing defects within β_1 are likely to create void volumes within the aggregate, which are expected to have profound consequences on the pressure stability of these entities. This thought has become a starting point for conducting high pressure experiments illustrated in Figure 4. High-pressure infrared (HP FT-IR) spectroscopy with diamond anvil cells allows one to collect *in situ* infrared spectra of protein dissolved in D₂O under pressure up to thousands of atmospheres.²⁹ We applied this method to monitor stability of β_2 and β_1 aggregates under high hydrostatic pressure at 25 °C (and also at 65 °C; see Supporting Information). As expected for a compact superstructure, the amide I' band of PLGA β_2 -aggregate remains virtually unaffected by pressure as high as 800 MPa (Figure 4A), although even moderately increased pressure causes reversible spectral changes in the region of the —COOD band (1731/1721 cm⁻¹) which is likely to reflect subtle elastic rearrangements of Glu side chains. This relatively pressure-insensitive behavior is in contrast to the case of the racemic PLGA + PDGA β_1 aggregate (panel B), wherein pressure as low as 200 MPa appears to cause pronounced shift of the main amide I' component from the β_1 position to that of the β_2 form. Simultaneously with the downshift of the 1613 cm⁻¹ band, high pressure causes attenuation of the 1683 cm⁻¹ peak and a less pronounced increase of absorption at around 1638 cm⁻¹. Pressure-induced changes in the spectral region of

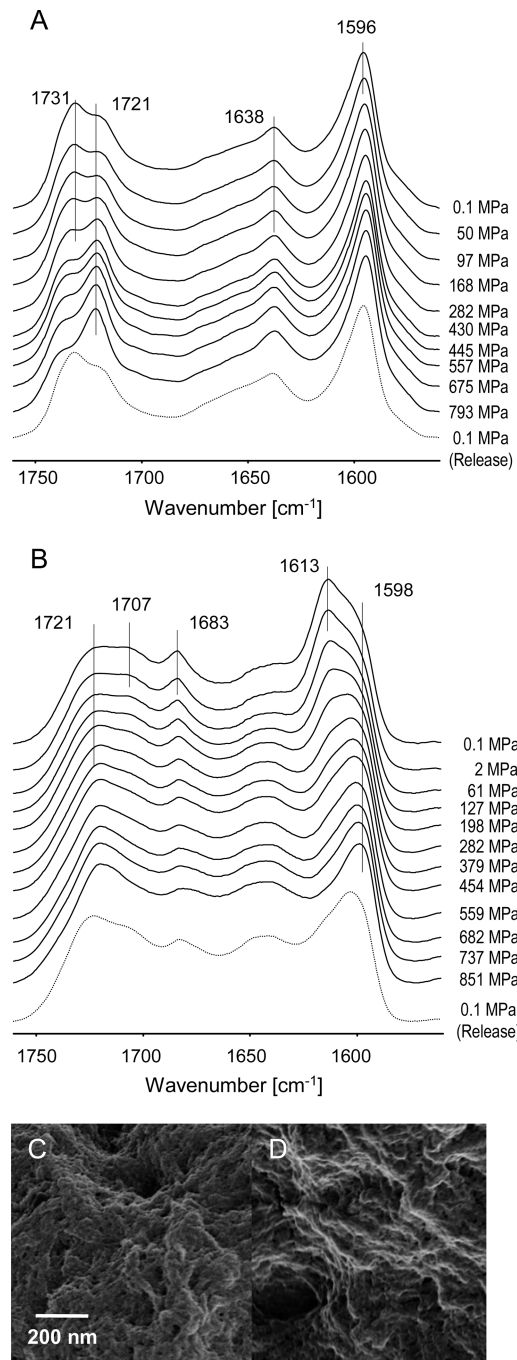


Figure 4. Effect of high hydrostatic pressure on FT-IR spectra of β_2 -aggregate from PLGA (A) and the aggregate obtained from racemic mixture of PLGA and PDGA (B). The high-pressure FT-IR spectra were collected at 25 °C using diamond anvil cell. SEM images of the PLGA + PDGA aggregate before (C) and after (D) 60 min incubation under 1 GPa hydrostatic pressure at room temperature.

Glu —COOD groups are more ambiguous. The distinct sharp 1731 cm⁻¹ peak of the β_2 form is absent in the infrared spectra of the racemic aggregates (Figure 2A), which exhibit only a broad and rather featureless plateau stretched between 1721 and 1707 cm⁻¹: an indication of heterogeneous and possibly unstructured surroundings of side chains. With the pressure increasing beyond 200 MPa, the band becomes narrower and centered around 1721 cm⁻¹ (Figure 4B). Thus, high pressure promotes the emergence of the 1721 cm⁻¹ peak in either β_2 or

β_1 aggregates (Figure 4A,B), but only in the former case pressure-released spectrum reverts to the ambient position at 1731 cm⁻¹. These observations suggest that the bifurcated hydrogen bonds causing the extreme downshift of the amide I' band involve —COOD groups in one of two spectrally distinguishable arrangements absorbing at 1731 or 1721 cm⁻¹. Assuming that local strains originating from packing defects or caused by high hydrostatic pressure give rise to the 1721 cm⁻¹ band, one could speculate that the 1731 cm⁻¹ peak stems from carboxyl groups in strain-free orderly packed fibrils. Certainly, further studies are needed before structural aspects and patterns of interactions underlying the fine features of the —COOD band could be explained in detail.

Although β_1 aggregate is, as aforementioned, metastable and does convert to β_2 even under ambient conditions (Figure 3A), such a transition is very slow. Therefore, the fast spectral changes observed in Figure 4B (with the steep pressure increase of 100 MPa/h) must be attributed to high pressure itself rather than to the slow time-dependent drift. As the final “release” spectrum acquired under atmospheric pressure indicates, the pressure-induced transition is quite irreversible at least in terms of several days (Supporting Information). This is distinct from the case of certain coiled-coil peptides also forming bifurcated HBs (albeit with surrounding water molecules as secondary hydrogen donors) under high pressure but in a reversible manner.^{30,32}

The racemic aggregate of poly(glutamic acid) revealed a very similar response to high pressure at 65 °C (Supporting Information). The strongly irreversible character of the transformation shown in Figure 4B suggests that high pressure (by causing collapse of void volumes) facilitates—rather unsurprisingly—crossing an activation barrier on the transition pathway from the less (β_1) to more (β_2) stable aggregate. Unfortunately, this irreversibility hampers calculation of reaction volumes of the transition, which could be otherwise attempted (Supporting Information). Since the high pressure treatment appears to “rescue” coaggregated PLGA and PDGA chains from the kinetic trap—at least in terms of local, (sub)conformational order and formation of bifurcated HBs—it was interesting to see whether that is accompanied by “mending” the aggregate on the superstructural level. However, SEM images collected for β_1 aggregates before (Figure 4C) and after (Figure 4D) high pressure treatment of 1 GPa suggest otherwise—the samples reveal similar degrees of amorphylicity. Moreover, the SEM data imply that an aggregate with β_2 -like infrared features may not form spiral superstructures such as shown in Figure 2. Because of extremely small sample volumes that may be subjected to high pressure treatment using accessible equipment (e.g., typical sample volume in a diamond anvil cell is less than 0.08 μ L), we were unable to collect and compare ThT fluorescence emission spectra before and after the pressure treatment. It could be hypothesized that in concentrated and viscous samples of β_1 subjected to high pressure treatment individual fibrils lack the reorientational freedom needed to assemble into spiral superstructures even if such a process was thermodynamically favored.

CONCLUSIONS

In summary, we have carried out a comparative study on stability of two types of amyloid-like aggregates formed by poly(glutamic acid) (i) built of chains of a single chiral component (PLGA or PDGA) and (ii) formed through coassembly of PLGA and PDGA. Our main findings concern

the observed influence of high pressure on the less ordered racemic aggregate of poly(glutamic acid) (β_1). There are known paradoxes of the pressure effects on aggregating (and already aggregated) proteins. High pressure may promote aggregation-prone protein conformations^{39–41} or enhance formation of early amyloid nuclei,⁴² but it also has the capacity to dissociate amyloid protofibrils.^{43,44} As the pressure sensitivity of an amyloid fibril depends on the presence of water-excluded cavities/void volumes within its walls, high pressure has become a useful parameter to study different stages of amyloidogenic self-assembly and polymorphism of amyloid fibrils.⁴⁵ Importantly, most of the existing studies suggest that the presence of structural defects will lead under high pressure to infiltration of protein aggregate by surrounding water molecules, followed by destabilization of protein–protein intermolecular bonds, and ultimately dissociation of the aggregate. In the case of β_1 aggregate, void volumes are too small to permit a significant structural disruption, while the absence of larger hydrophobic clusters and salt bridges disfavors alternative scenarios for pressure-induced dissociation.

According to our study, high pressure may correct folding defects on conformational and subconformational scales in amyloid-like fibrils composed of poly(glutamic acid). This shows that hyperbaric investigations may provide insightful means to explore such defects and particular interactions requiring well-ordered packing of neighboring polypeptide chains, as is the case of three-center hydrogen bonds in β_2/β_1 aggregates. Further work is needed before high pressure could become a synthetic route to defect-free and highly homogeneous fibrous bionanomaterials.

ASSOCIATED CONTENT

S Supporting Information

Additional Raman and high-pressure FT-IR data and analysis; SEC analysis of PLGA. This material is available free of charge via the Internet at <http://pubs.acs.org>.

AUTHOR INFORMATION

Corresponding Author

*Phone +48 22 8220211 ext 528; Fax +48 22 822 5996; e-mail wdzwolak@chem.uw.edu.pl.

Notes

The authors declare no competing financial interest.

ACKNOWLEDGMENTS

We are grateful to Dr. Grzegorz Łapienis for SEC measurements and to Mr. Adam Presz for his kind help with SEM measurements. This work was supported by the Polish Ministry of Education and Science (grant NN 301 101236 to W.D.).

ABBREVIATIONS

AFM, atomic force microscopy; FT-IR, Fourier transform infrared; HB, hydrogen bond; HP, high pressure; MW, molecular weight; PDGA, poly(D-glutamic acid); PLGA, poly(L-glutamic acid); SEC, size exclusion chromatography; SEM, scanning electron microscopy; TEM, transmission electron microscopy; ThT, Thioflavin T.

REFERENCES

- (1) Chiti, F.; Dobson, C. M. *Annu. Rev. Biochem.* **2006**, 75, 333.
- (2) Fändrich, M.; Fletcher, M. A.; Dobson, C. M. *Nature* **2001**, 410, 165.

- (3) Chiti, F.; Webster, P.; Taddei, N.; Clark, A.; Stefani, M.; Ramponi, G.; Dobson, C. M. *Proc. Natl. Acad. Sci. U. S. A.* **1999**, *96*, 3590.
- (4) Herczenik, E.; Gebbink, M. F. B. G. *FASEB J.* **2008**, *22*, 2115.
- (5) Smith, A. M.; Scheibel, T. *Macromol. Chem. Phys.* **2010**, *211*, 127.
- (6) Maji, S. K.; Perrin, M. H.; Sawaya, M. R.; Jessberger, S.; Vadodaria, K.; Rissman, R. A.; Singru, P. S.; Nilsson, K. P. R.; Simon, R.; Schubert, D.; Eisenberg, D.; Rivier, J.; Sawchenko, P.; Vale, W.; Riek, R. *Science* **2009**, *325*, 328.
- (7) Fowler, D. M.; Koulov, A. V.; Alory-Jost, C.; Marks, M. S.; Balch, W. E.; Kelly, J. W. *PLoS Biol.* **2006**, *4*, 0100.
- (8) Scheibel, T.; Parthasarathy, R.; Sawicki, G.; Lin, X.-M.; Jaeger, H.; Lindquist, S. L. *Proc. Natl. Acad. Sci. U. S. A.* **2003**, *100*, 4527.
- (9) Reches, M.; Gazit, E. *Science* **2003**, *300*, 625.
- (10) Wojcik, S.; Babenko, V.; Dzwolak, W. *Langmuir* **2010**, *26*, 18303.
- (11) MacPhee, C. E.; Woolfson, D. N. *Curr. Opin. Solid State Mater. Sci.* **2004**, *8*, 141.
- (12) Fändrich, M.; Dobson, C. M. *EMBO J.* **2002**, *21*, 5682.
- (13) Dzwolak, W.; Ravindra, R.; Nicolini, C.; Jansen, R.; Winter, R. J. *Am. Chem. Soc.* **2004**, *126*, 3762.
- (14) Guo, Y.; Ma, Y.; Xu, L.; Li, J.; Yang, W. *J. Phys. Chem. C* **2007**, *111*, 9172.
- (15) Guan, J.; Li, J.; Guo, Y.; Yang, W. *Langmuir* **2009**, *25*, 2679.
- (16) Itoh, K.; Foxman, B. M.; Fasman, G. D. *Biopolymers* **1976**, *15*, 419.
- (17) Fulara, A.; Dzwolak, W. *J. Phys. Chem. B* **2010**, *114*, 8278.
- (18) Fulara, A.; Lakhani, A.; Wójcik, S.; Nieznaska, H.; Keiderling, T. A.; Dzwolak, W. *J. Phys. Chem. B* **2011**, *115*, 11010.
- (19) Foguel, D.; Suarez, M. C.; Ferrao-Gonzales, A. D.; Porto, T. C. R.; Palmieri, L.; Einsiedler, C. M.; Andrade, L. R.; Lashuel, H. A.; Lansbury, P. T.; Kelly, J. W.; Silva, J. L. *Proc. Natl. Acad. Sci. U. S. A.* **2003**, *100*, 9831.
- (20) Dirix, C.; Meersman, F.; MacPhee, C. E.; Dobson, C. M.; Heremans, K. *J. Mol. Biol.* **2005**, *347*, 903.
- (21) Mishra, R.; Winter, R. *Angew. Chem., Int. Ed.* **2008**, *47*, 6518.
- (22) Radovan, D.; Smirnovas, V.; Winter, R. *Biochemistry* **2008**, *47*, 6352.
- (23) Dubois, J.; Ismail, A. A.; Chan, S. L.; Ali-Khan, Z. *Scand. J. Immunol.* **1999**, *49*, 376.
- (24) Brown, P.; Meyer, R.; Cardone, F.; Pocchiari, M. *Proc. Natl. Acad. Sci. U. S. A.* **2003**, *100*, 6093.
- (25) Moustaine, D. E.; Perrier, V.; Van Ba, S. A.-T.; Meersman, F.; Ostapchenko, V. G.; Baskakov, I. V.; Lange, R.; Torrent, J. *J. Biol. Chem.* **2011**, *286*, 13448.
- (26) Jansen, R.; Grudzielanek, S.; Dzwolak, W.; Winter, R. *J. Mol. Biol.* **2004**, *338*, 203.
- (27) Knowles, T. P. J.; Buehler, M. J. *Nat. Nanotechnol.* **2011**, *6*, 469.
- (28) Dzwolak, W.; Lokszejn, A.; Smirnovas, V. *Biochemistry* **2006**, *45*, 8143.
- (29) Dzwolak, W.; Kato, M.; Taniguchi, Y. *Biochim. Biophys. Acta* **2002**, *1595*, 131.
- (30) Imamura, H.; Isogai, Y.; Takekiyo, T.; Kato, M. *Biochim. Biophys. Acta* **2010**, *1804*, 193.
- (31) Imamura, H.; Kato, M. *Proteins* **2009**, *75*, 911.
- (32) Segawa, Y.; Imamura, H.; Shimizu, A.; Kato, M. *J. Phys. Conf. Ser.* **2010**, *215*, 012154.
- (33) Groenning, M. *J. Chem. Biol.* **2010**, *3*, 1.
- (34) Stsiapura, V. I.; Maskevich, A. A.; Kuzmitsky, V. A.; Turoverov, K. K.; Kuznetsova, I. M. *J. Phys. Chem. A* **2007**, *111*, 4829.
- (35) Maskevich, A. A.; Stsiapura, V. I.; Kuzmitsky, V. A.; Kuznetsova, I. M.; Povarova, O. I.; Uversky, V. N.; Turoverov, K. K. *J. Proteome Res.* **2007**, *6*, 1392.
- (36) Dzwolak, W.; Pecul, M. *FEBS Lett.* **2005**, *579*, 6601.
- (37) Babenko, V.; Dzwolak, W. *Chem. Commun.* **2011**, *47*, 10686.
- (38) Gilmanshin, R.; Williams, S.; Callender, R. H.; Woodruff, W. H.; Dyer, R. B. *Biochemistry* **1997**, *36*, 15006.
- (39) Ferrão-Gonzales, A. O.; Souto, S. O.; Silva, J. L.; Foguel, D. *Proc. Natl. Acad. Sci. U. S. A.* **2000**, *97*, 6445.
- (40) Smeller, L.; Rubens, P.; Heremans, K. *Biochemistry* **1999**, *38*, 3816.
- (41) Meersman, F.; Dobson, C. M.; Heremans, K. *Chem. Soc. Rev.* **2006**, *35*, 908.
- (42) Grudzielanek, S.; Zhai, Y.; Winter, R. *ChemPhysChem* **2010**, *11*, 2016.
- (43) Kamatari, Y. O.; Yokoyama, S.; Tachibana, H.; Akasaka, K. *J. Mol. Biol.* **2005**, *349*, 916.
- (44) Akasaka, K.; Latif, A. R. A.; Nakamura, A.; Matsuo, K.; Tachibana, H.; Gekko, K. *Biochemistry* **2007**, *46*, 10444.
- (45) Foguel, D.; Silva, J. L. *Biochemistry* **2004**, *43*, 11361.